JOURNAL OF OPTOELECTRONICS AND ADVANCED MATERIALS, Vol. 11, No. 1, January 2008, p. 1 - 14

Review Paper

Light-induced defect creation under intense pulsed illumination in hydrogenated amorphous silicon

K. MORIGAKI *, H. HIKITA[a], C. OGIHARA[b]
Department of Electrical and Digital-System Engineering, Hiroshima Institute of Technology, Miyake, Saeki-ku, Hiroshima 731-5193, Japan
** Present address: C-305 Wakabadai 2-12, Inagi, Tokyo 206-0824, Japan.*
[a] Physics Laboratory, Meikai University, Urayasu, Chiba 279-8550, Japan
[b] Department of Applied Science, Yamaguchi University, Ube 755-8611, Japan

Some experimental results taken from the literatures on the kinetics of light-induced defect creation observed under intense pulsed illumination in hydrogenated amorphous silicon (a-Si:H) are reviewed and are discussed in terms of our model. The deconvolution of the ESR line into two components due to normal dangling bonds and hydrogen-related dangling bonds is performed and is compared with their spin density ratio calculated from our model, being consistent with our model. The relationships of the dispersion parameter, β, and the characteristic time, τ, vs. the generation rate of free carriers are discussed, being also consistent with our model. Related defects, i.e., hydrogen-related dangling bonds, self-trapped holes and hydrogen-pairs, are discussed.

(Received October 6, 2008; accepted January 21, 2009)

Keywords: Amorphous hydrogenated silicon, Defect, ESR, Radiation effect

1. Introduction

Light-induced degradation of electronic properties of hydrogenated amorphous silicon (a-Si:H) and performance of amorphous silicon solar cells have attracted much attention from viewpoints of physics and application during more than three decades [1-7]. The origin of such degradation has been found to be due to light-induced creation of dangling bonds [8, 9], but the mechanism for light-induced defect creation is still a controversial issue although many researchers have attempted to elucidate it by proposing different models [1-7, 10-19]. Typical models are the bond-breaking model by Stutzmann et al. [10] and Branz (so-called hydrogen-collision model) [15, 18]. Our model [19] is also based on the bond-breaking model. In this paper, we treat light-induced defect creation under intense pulsed illumination in a-Si:H. This type of illumination creating dangling bonds of more than 10^{18} cm^{-3} is in contrast with continuous illumination giving rise to dangling bonds of $\sim 10^{17}$ cm^{-3}. We have proposed a model for light-induced defect creation under continuous illumination in a-Si:H[19] and have extended it to the case of intense pulsed illumination [20, 21]. Typical experiments of Tzanetakis et al. [22] and Stutzmann et al. [23] done under intense pulsed illumination are reviewed as well as our experiment [21] in this paper. We have already reported on comparison of calculated results by our model with the results of our electron spin resonance (ESR) measurement under pulsed illumination at 10 K [21]. We used a YAG optical parametric oscillator laser system as a pulsed light source, in which pulsed light had a width of 10 ns, a repetition frequency of 11 Hz and a power density of 100 $mJcm^{-2}$ operating at either 2.48 eV (500 nm) or 1.55 eV (800 nm). The light-induced dangling bond density reaches at 1.1×10^{19} cm^{-3} in a-Si:H illuminated for 3 h with the above pulsed laser light at 2.48 eV (500 nm) with $G = 3.8 \times 10^{30}$ $s^{-1}cm^{-2}$. In this paper, we summarize the above experiment and present the result of deconvolution of the ESR line observed under intense pulsed illumination. Further, we consider the ESR line observed by Stutzmann et al. [23] under intense pulsed illumination along with comparison between the result of deconvolution of the ESR line and our calculated result by our model [19-21].

First, we present our model for light-induced defect creation under intense pulsed illumination in a-Si:H. Second, we present calculated results by our model for three experiments mentioned above and compare them with the experimental results. Further, we present the result of the shape of the ESR line due to dangling bonds in a-Si:H. Third, we discuss the kinetics of light-induced defect creation under intense pulsed illumination, the nature of related defects, i.e., self-trapped holes, hydrogen-related dangling bonds and hydrogen pairs. Further, we comment about the so-called microscopic constraint for the mechanism of light-induced defect creation in a-Si:H. Finally, conclusions are presented.

2. Model

The processes involved in light-induced defect creation under illumination in a-Si:H are given as follows[19]: A hole is self-trapped in a specific weak Si-Si bond that is a weak Si-Si bond adjacent to a Si-H bond (Fig. 1(a)) and then is recombined with an electron most

nonradiatively (Fig.1(b)) and eventually the weak bond is broken. Using the recombination energy associated with nonradiative recombination between the electron and the hole, the Si-H bond is switched towards the weak Si-Si bond (Fig. 1(c)).

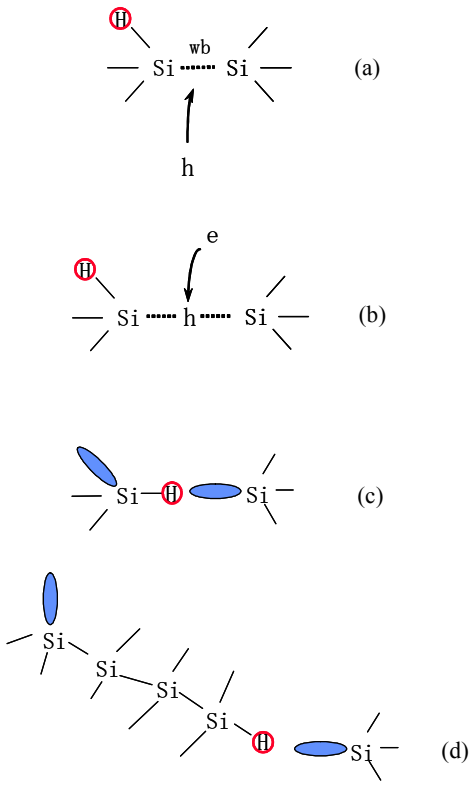

Fig. 1. Atomic configurations involved in the formation of two types of dangling bonds, i.e., normal dangling bonds and hydrogen-related dangling bonds, under illumination: (a) Self-trapping of a hole in a weak Si-Si bond (wb) adjacent to a Si-H bond, (b) Electron-hole recombination at a weak Si-Si bond, (c) Switching of a Si-H bond towards the weak Si-Si bond, leaving a dangling bond behind, (d) Formation of two separate dangling bonds through hydrogen movement after repeating the processes shown in (a) – (c).

After switching of the Si-H bond (Fig. 1(c)) and breaking of the weak Si-Si bond, the two close dangling bonds created are separated by movement of hydrogen due to hopping and/or tunneling (Fig. 1(d)) and eventually two separate dangling bonds (Fig. 1(d)), i.e., a normal dangling bond and a hydrogen-related dangling bond, that is a dangling bond having hydrogen at the nearby site, are created under illumination, as shown in Fig. 1(d). Hydrogen is dissociated from a Si-H bond located near a hydrogen-related dangling bond as a result of nonradiative recombination between an electron and a hole at the hydrogen-related dangling bond. A dissociated hydrogen atom (metastable hydrogen atom) is inserted into a nearby weak Si-Si bond to form a hydrogen-related dangling bond. A dissociated hydrogen atom also terminates either a normal dangling bond or a hydrogen-related dangling bond. A dissociated hydrogen atom has a chance to form a hydrogen molecule by meeting together. These processes are depicted in Fig. 2.

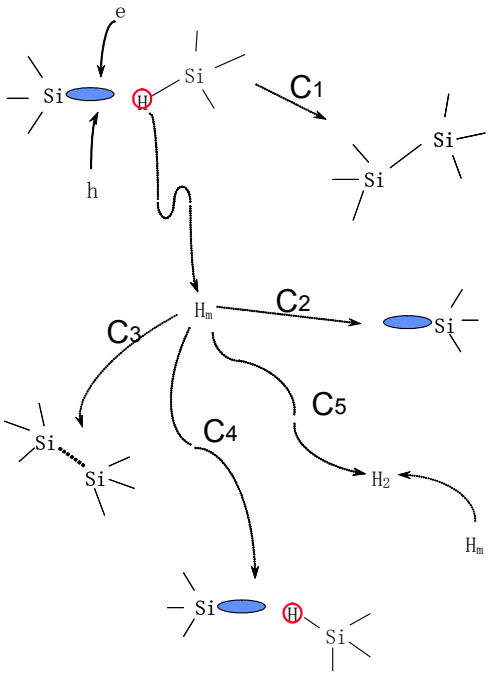

Fig. 2. Illustrations for reactions: C_1, C_2, C_3, C_4 and C_5. See the text for definitions of these parameters.

The light-induced defect creation is considered in terms of a rate-equation model, taking into account the processes mentioned above. Rate equations are given as follows:

$$dN_a/dt = C_d np(N_w/N_{w0}) - C_2 N_m N_a, \quad (1)$$

$$dN_b/dt = C_d np(N_w/N_{w0}) - C_1 np N_b + C_3 N_m N_{Si} - C_4 N_m N_b, \quad (2)$$

$$dN_m/dt = C_1 np N_b - C_2 N_m N_a - C_3 N_m N_{Si} - C_4 N_m N_b - C_5 N_m^2, \quad (3)$$

$$dN_w/dt = - C_d np(N_w/N_{w0}) + C_2 N_m N_a + C_4 N_m N_b, \quad (4)$$

where N_a, N_b, N_m, N_{Si}, N_w, N_{w0}, n and p are densities of normal dangling bonds, hydrogen-related dangling bonds, metastable hydrogen atoms, Si-Si bonds, weak Si-Si bonds adjacent to a Si-H bond, N_w at t = 0, free electrons and free holes including band-tail-electrons and -holes, respectively and C_d, C_1, C_2, C_3, C_4 and C_5 are reaction coefficients of the following processes. The processes of C_1, C_2, C_3, C_4 and C_5 are illustrated in Fig. 2: C_d the light-induced creation of two separate dangling bonds, C_1 the dissociation of a hydrogen atom from a Si-H bond located near a hydrogen-related dangling bond, C_2 the termination of a normal dangling bond by a metastable hydrogen atom, C_3 the insertion of a metastable hydrogen atom into a Si-Si bond, C_4 the termination of a hydrogen-related dangling bond by a metastable hydrogen atom and C_5 the formation of a hydrogen molecule by two metastable hydrogen atoms, respectively. In Eq. (4), the density of weak Si-Si bonds decreases with formation of dangling bonds and increases with termination of dangling bonds by hydrogen atoms, because a Si-Si bond adjacent to a Si-H

bond is considered to become a weak bond. For high-quality a-Si:H, the C_3 term is neglected, because the density of weak Si-Si bonds is relatively small compared to low-quality a-Si:H containing a large amount of hydrogen. In numerical calculations, the C_5 term is also neglected for simplicity.

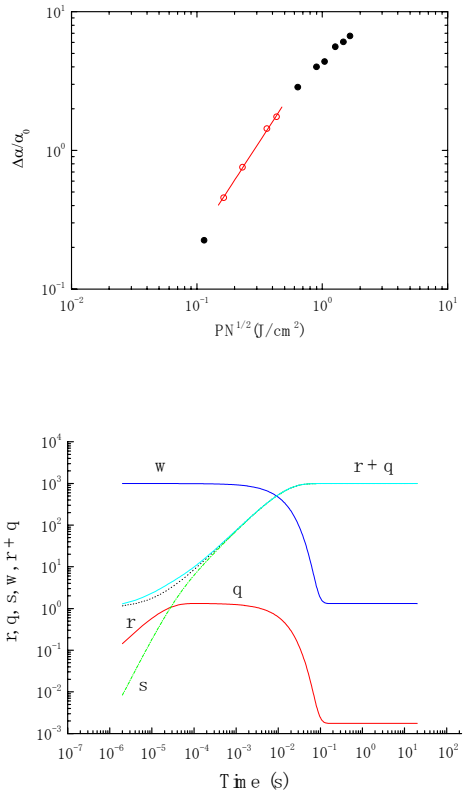

Fig. 3(a). Relative change in subgap absorption $\Delta\alpha$ / α_0 as a function of the product of P (= 5.2 mJ/cm^2/pulse) and $N^{1/2}$, in which P and N are the power per pulse and the number of pulse, respectively (cited from Tzanetakis et al. [22]). The solid line is a least-square fit of four experimental points (open circles) at small values except a smallest point. (b) Calculated densities of total dangling bonds, r + q (solid line), normal dangling bonds, r (dotted line), hydrogen-related dangling bonds, q (solid line), metastable hydrogen atoms, s (dot-dashed line), and weak Si-Si bonds, w (solid line), relative to N_{d0} = 1 × 10^{16} cm^{-3} as a function of total exposure time for the case of Tzanetakis et al. [22]. See the text for detail.

First, we consider the case of relatively weak illumination such as continuous illumination[19]. In this case, we neglect Eq. (4), because the weak Si-Si bond exists much more than light-induced dangling bonds, e.g., $N_w \cong 10^{19}$ cm^{-3} and $N_d \cong 10^{17}$ cm^{-3} , so that the density of weak Si-Si bonds under illumination is assumed not to be changed.

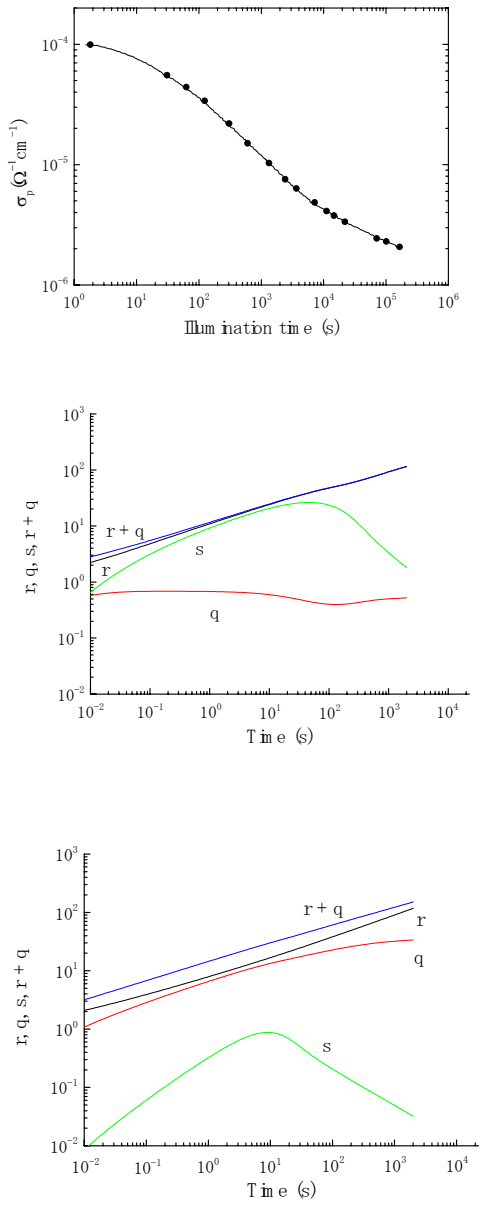

Fig. 4(a). σ_p vs. illumination time at 300 K under pulsed illumination by a Xe-flash lamp with 2 μs width, a repetition frequency of 300 Hz and an average power of 150 W/cm^2 for a 2.5 μm thick a-Si:H film (cited from Stutzmann et al. [23]). (b) and (c) Calculated densities of total dangling bonds, r + q (solid line), normal dangling bonds, r (dotted line), hydrogen-related dangling bonds, q (solid line), metastable hydrogen atoms, s (dot-dashed line), and weak Si-Si bonds, w (solid line), relative to N_{d0} = 1 × 10^{16} cm^{-3} as a function of total exposure time for the case of Stutzmann et al. [23]. (b): A_1 = 756 s^{-1}, (c): A_1 = 7.56 s^{-1}. The values of other parameters are the same for (b) and (c). See the text for detail.

The carrier densities n and p are assumed to be determined by their steady-state values and by trapping of carriers (electrons) at neutral dangling bonds followed by rapid recombination with holes, and then they are proportional to G/N_d, where G and N_d are the generation rate of free carriers and the total density of neutral dangling bonds, respectively, because the trapping process at neutral dangling bonds of carriers in the conduction band and its tail states occurs faster than the kinetics of light-induced creation of dangling bonds. The steady-state values of n and p are approximately

$$n = p \cong G/(\alpha N_d) \tag{5}$$

where α is the trapping coefficient of free carriers by neutral dangling bonds. Then, in order to solve the rate equation numerically, the rate equations (1) – (3) are rewritten, using normalized densities of N_a, N_b, and N_m to N_{d0} ($\equiv N_d$ (t = 0)), i.e., r, q, and s, respectively, as follows:

$$dr/dt = A/(r+q)^2 - A_2sr, \tag{6}$$
$$dq/dt = A/(r+q)^2 - A_1q/(r+q)^2 + A_3s - A_4sq, \tag{7}$$
$$ds/dt = A_1q/(r+q)^2 - A_2sr - A_3s - A_4sq - A_5s^2, \tag{8}$$
$$r = N_a/N_{d0}, \tag{9} \quad q = N_b/N_{d0}, \tag{10} \quad s = N_m/N_{d0}, \tag{11}$$
$$N_d = N_a + N_b, \tag{12}$$
$$A = C_dG^2/\alpha^2N_{d0}^3, \tag{13}$$
$$A_1 = C_1G^2/\alpha^2N_{d0}^2, \tag{14}$$
$$A_2 = C_2N_{d0}, \tag{15}$$
$$A_3 = C_3N_{Si}, \tag{16}$$
$$A_4 = C_4N_{d0}, \tag{17}$$
$$A_5 = C_5N_{d0}, \tag{18}$$

Second, we consider the case of intense illumination[19, 20]. Under this condition, the carrier densities n and p are determined by bimolecular recombination, i.e., recombination between an electron and a hole created by light, and their steady-state values given below are used in rate-equations because the recombination occurs faster than the kinetics of the light-induced creation of dangling bonds.

The steady-state values of n and p are approximately

$$n = p \cong (G/\beta)^{1/2}, \tag{19}$$

where β is the recombination coefficient of free electrons (or tail electrons) and free holes (or tail holes), respectively. Then, the rate equations of (1) – (4) are rewritten to solve them numerically as follows:

$$dr/dt = B_0w - B_2sr, \tag{20}$$
$$dq/dt = B_0w - B_1q + B_3s - B_4sq, \tag{21}$$
$$ds/dt = B_1q - B_2sr - B_3s - B_4sq - B_5s^2, \tag{22}$$
$$dw/dt = -B_0w + B_2sr + B_4sq, \tag{23}$$
$$w = N_w/N_{d0}, \tag{24}$$
$$B_0 = C_dG/\beta N_{d0}w_0 \ (w_0 = w \text{ at } t = 0), \tag{25}$$
$$B_1 = C_1G/\beta, \tag{26}$$
$$B_2 = C_2N_{d0}, \tag{27}$$
$$B_3 = C_3N_{Si}, \tag{28}$$
$$B_4 = C_4N_{d0}, \tag{29}$$
$$B_5 = C_5N_{d0}, \tag{30}$$

where r, q, s and N_d are given by Eqs. (9), (10), (11) and (12). B_2, B_3, B_4 and B_5 are the same as A_2, A_3, A_4 and A_5, respectively, where A_2, A_3, A_4 and A_5 are the reaction coefficients defined in the monomolecular recombination case, where N_{d0} is N_d at t = 0. In the calculation for pulsed illumination, the optical excitation of pulsed light is approximated by the continuous illumination, taking the total exposure time by pulsed light as the illumination time, because the rate equations involving pulsed optical excitation are not easy to be solved numerically. This is justified within an ambiguity of a factor of about 0.74 for the calculated light-induced defect density by citing the results of Stradins et al.[24] in which they measured the defect creation efficiency for pulsed illumination as a function of the separation time of two laser pulses. Thus, numerical calculations are performed, using rate equations (20) – (23), under continuous illumination. The results are compared with experimental ones performed under pulsed illumination in the following section.

3. Results

For the literatures concerning pulsed light-soaking on a-Si:H, we cite an experiment of Tzanetakis et al.[22] estimating the relative light-induced change in subgap absorption, $\Delta\alpha / \alpha_0$ (α : absorption coefficient, $\alpha = \alpha_0$ at t = 0) by constant photocurrent measurement (CPM) and an experiment of Stutzmann et al. [23] estimating the relative change in photoconductivity. Further, we consider ESR experiments on high-quality a-Si:H film under intense pulsed illumination[21, 23], as mentioned in Section 1.

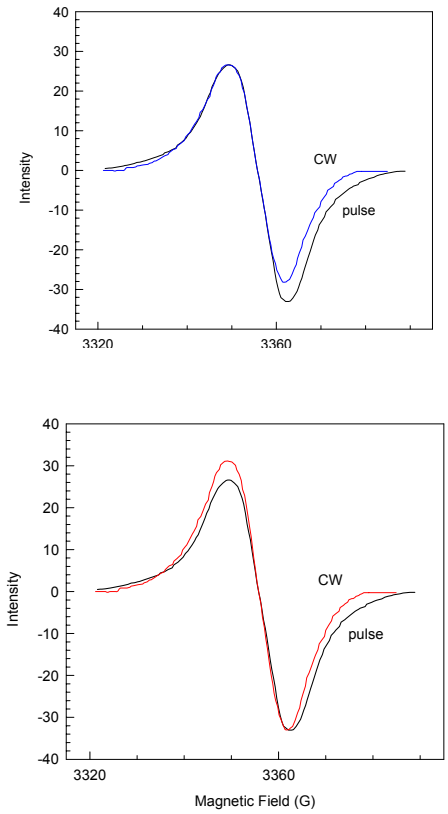

Fig. 5. ESR spectra observed by Stutzmann et al. [23] after 4 h of continuous (CW) illumination and after 2 h of illumination with a pulsed colliding pulse mode-locked laser (Pulse)(cited from Stutzmann et al. [23]). The average power and temperature are 300 W/ cm^2 and 300 K, respectively. The low-magnetic field peak of ESR absorption derivative (a) and the high-magnetic field peak of ESR absorption derivative (b) are normalized for comparison of two spectra CW and Pulse, respectively.

Tzanetakis et al.[22] observed the exposure-time dependence of $\Delta\alpha$ / α_0 for a-Si:H, using pulsed illumination of 5.2 mJ/cm^2/pulse (= 1.7 × 10^{16}/cm^2/pulse) at 1.91 eV and a repetition frequency of 7 – 10 Hz as follows: When the value of $PN^{1/2}$, in which P (= 5.2 mJ/cm^2/pulse) and N are the power per pulse and the number of pulse, respectively, is in the range of 0.1 and 1, the slope γ is 0.67 for an overall least-square fit (see Fig. 1 in ref. [22]) and 0.70 for a least-square fit with four experimental points, as shown in Fig. 3(a), where γ is defined as $\Delta\alpha / \alpha_0 \propto t^{\gamma}$ ($t \propto N$). These values of $PN^{1/2}$ correspond to exposure time of 1.1 × 10^{-4} s and 1.1 × 10^{-3} s, respectively. This result can be almost realized by taking the values of parameters[19] in Eqs. (25) – (30) shown in Table 1. Concerning the choice of the values of parameters, see ref.[19]. Further we use the relationship of $\beta = 3\alpha$ [23]. We assume that the dangling bonds before illumination are only normal dangling bonds, i.e., $r_0 = 1.0$, $q_0 = 0$. Then, we have $B_0 = 76\ s^{-1}$, $B_1 = 5.7 \times 10^4\ s^{-1}$, $B_2 = 1 \times 10^{-4}\ s^{-1}$, $B_3 = 0$, $B_4 = 1 \times 10^{-2}\ s^{-1}$, and $B_5 = 0$. The calculated r + q vs. t curve is shown in Fig. 3(b), where the slope of the log(r + q) vs. log t curve is 0.81 in the above range of t. The calculated slope is compared with the least-square fit taking experimental points at small $PN^{1/2}$ values shown in Fig. 3(a), because the overall least-square fit seems to us inappropriate since the experimental points at high $PN^{1/2}$ values tend to lean the slope towards saturation. The calculated slope, i.e., 0.81, is close to the observed one, i.e., 0.70.

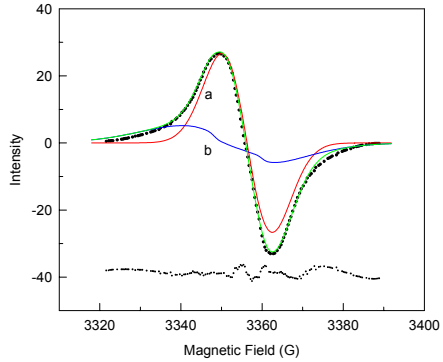

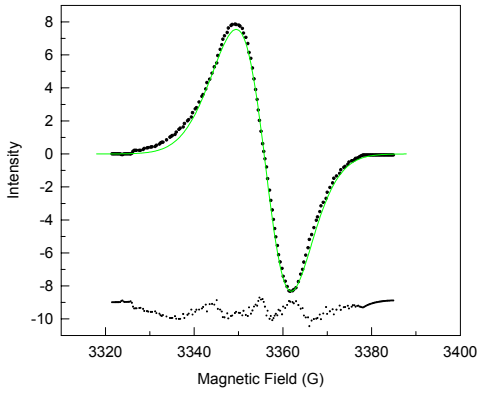

Fig. 6. Deconvolution of the observed ESR spectrum into two components due to normal dangling bonds a and hydrogen-related dangling bonds b in a light-soaked a-Si:H sample with pulsed illumination shown in Fig. 5 (cited from Stutzmann et al. [23]). The solid points and the solid curve are the observed ESR spectrum and a superposition of dashed curves a and b, respectively. The residual between the calculated ESR spectrum and the observed ESR spectrum is shown in the lower part of the figure with a scale twice extended compared to other curves. (a) Pulse in Fig. 5: Two components a and b are taken into account. (b) CW in Fig. 5: Only a component due to normal dangling bonds is taken into account. See the text for detail.

Stutzmann et al.[23] have measured the illumination time-dependence of photoconductivity under pulsed illumination by a Nd-YAG pumped optical parametric oscillator (OPO) and also by a Xe flash lamp. The photoconductivity, σ_p, may be anti-correlated with spin density, N_s , such as $\sigma_p \propto N_s^{-1}$ in the monomolecular recombination case. Indeed, they measured a relationship between σ_p and N_s obtained from ESR measurements and found that this is the case for pulsed illumination by a Xe flash lamp for a 0.5 μm thick sample. Thus, we compare the σ_p results (Fig. 4(a)) for this illumination with calculated results taking the monomolecular recombination case, as shown below. Judging from the observed result of the linear dependence of σ_p^{-1}on N_s, comparison between calculation and experiment can be done for σ_p between 10^{-6} Ω^{-1}cm^{-1}and 10^{-5} Ω^{-1}cm^{-1}corresponding to illumination time of more than 1.46×10^3 s that is total exposure time of 0.875 s (note that illumination time includes the interval of successive pulses)(see Fig. 4(a)). The values of parameters used in the calculation are given as follows: $G = 5 \times 10^{24}$ cm^{-3}s^{-1}, r_0= 1.0, q_0=0, A=520 s^{-1}, A_1=756 s^{-1}, A_2=1 ×10^{-4} s^{-1}, A_3= 0, A_4=1 ×10^{-2} s^{-1}, A_5=0, $\alpha = 1 \times 10^{-8}$ cm^{3}s^{-1} and N_{d0}= 1 × 10^{16} cm^{-3}, where the values of parameters, C_d, C_1, C_2, C_3, C_4 and C_5 are taken to be the same as those [19] for continuous illumination by Stutzmann et al.[10], as shown in Table 1. The calculated result is shown in Fig. 4 (b).

Table 1 The values of parameters used in the calculation for each figure.

Measurement	Calculation	C_d (cm^{3}s^{-1})	C_1(cm^{6}s^{-1})	C_2(cm^{3}s^{-1})	C_3(cm^{3}s^{-1})	C_4(cm^{3}s^{-1})	C_5(cm^{3}s^{-1})	α,β(cm^{3}s^{-1})	N_{d0}(cm^{-3})	G(cm^{-3}s^{-1})
Tzanetakis et al.[22]	Fig. 3(b)	4×10^{-15}	3×10^{-31}	1×10^{-20}	0	1×10^{-18}	0	β=3×10^{-8}	1×10^{16}	5.7×10^{27}
Stutzmann et al.[23]	Fig. 4(b)	2×10^{-15}	3×10^{-31}	1×10^{-20}	0	1×10^{-18}	0	α=1×10^{-8}	1×10^{16}	5×10^{24}
Stutzmann et al.[23]	Fig. 4(c)	2×10^{-15}	3×10^{-33}	1×10^{-20}	0	1×10^{-18}	0	α=1×10^{-8}	1×10^{16}	5×10^{24}
Stutzmann et al.[23]	Fig. 7	2×10^{-15}	3×10^{-33}	1×10^{-20}	0	1×10^{-18}	0	β=3×10^{-8}	1×10^{16}	2.67×10^{30}
Morigaki et al.[21]	Fig. 8	4×10^{-14}	3×10^{-31}	1×10^{-31}	0	1×10^{-18}	0	β=3×10^{-8}	1×10^{16}	2×10^{27}
Morigaki et al.[21]	Fig. 9	4×10^{-15}	3×10^{-31}	1×10^{-31}	0	1×10^{-18}	0	β=3×10^{-8}	1×10^{16}	3.8×10^{30}
Morigaki et al.[21]	Fig. 12	4×10^{-14}	3×10^{-31}	1×10^{-31}	0	1×10^{-18}	0	β=3×10^{-8}	1×10^{16}	2×10^{25}
Morigaki et al.[21]	Fig. 13	4×10^{-15}	3×10^{-31}	1×10^{-31}	0	1×10^{-18}	0	β=3×10^{-8}	1×10^{16}	3.8×10^{24}
$r_0 = 1$, $q_0 = 0$, $s_0 = 0$, $w_0 = 10^3$, β = 3α [23]										

As shown in Fig. 4(b), the slope of the log (r + q) vs. log t (total exposure time) curve is 0.32 below 80 s, while the observed slope of the log σ_p vs. log t curve by Stutzmann et al.[23] below 100 s changes around 6 s of total exposure time (10^4 s of illumination time) from 0.48 to 0.24 (see Fig. 4(a)). Using the σ_p^{-1} vs. N_s diagram measured by Stutzmann et al. [23], the log σ_p vs. log t curve can be transformed into the log N_s vs. log t curve whose slope is 0.38 and 0.32 below and above total exposure time of 1.3 s, respectively. The calculated curve should be compared with the log N_s vs. log t curve . The slopes of both curves are similar to each other, but the calculated curve exhibits a single slope of 0.32 below 80 s, while the observed curve exhibits two slopes with slightly different values of 0.38 below 1.3 s and 0.32 above 1.3 s, as mentioned above. The observed value of N_s by Stutzmann et al. [23] for illumination time of 3.2×10^4 s (total exposure time of 19.2 s) is 3×10^{17} cm^{-3}, being in an exact agreement with the calculated value, 3.0×10^{17} cm^{-3}.

In order to explore a different calculated curve, we take a different value of C_1 shown in Table 1, i.e., A_1, as follows: A_1 = 7.56 s^{-1} and the same values of the other parameters as the above values. The reaction coefficient C_1 is two orders of magnitudes smaller than the above value. The calculated curves are shown in Fig. 4(c). The value of r + q gradually increases with increasing t and two slopes are seen with the values of 0.32 and 0.30 below and above 10 s, respectively. Thus, the calculated r + q vs. t curve exhibits a different behaviour from the observed one. The calculated value of N_s at the total exposure time of 19.2 s

is 3.7 × 10^{17} cm^{-3}, being in a good agreement with the observed value, 3 × 10^{17} cm^{-3} [23]. However, it seems to us difficult to obtain an exact agreement between calculation and experiment for the r + q vs. t curve.

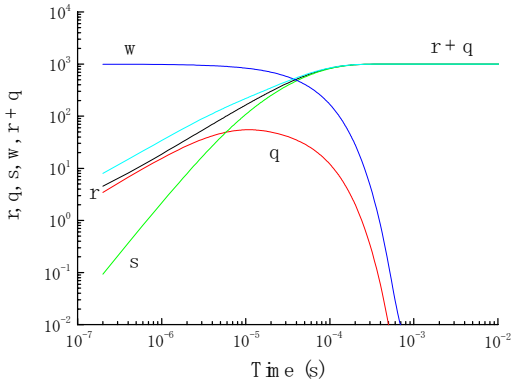

Fig. 7. Densities of total dangling bonds, r + q (solid line), normal dangling bonds, r (dotted line), hydrogen-related dangling bonds, q (solid line), metastable hydrogen atoms, s (dot-dashed line), and weak Si-Si bonds, w (solid line), relative to N_{d0} = 1 × 10^{16} cm^{-3} as a function of total exposure time under illumination with G = 2.67 × 10^{30} $cm^{-3}s^{-1}$. For the values of parameters, see text. The saturated dangling bond density of 1 × 10^{19} cm^{-3} is shown in the figure.

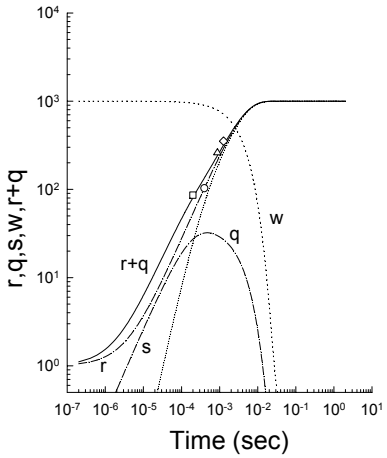

Fig. 8. Densities of total dangling bonds, r + q (solid line), normal dangling bonds, r (dotted line), hydrogen-related dangling bonds, q (solid line), metastable hydrogen atoms, s (dot-dashed line), and weak Si-Si bonds, w (solid line), relative to N_{d0} = 1 × 10^{16} cm^{-3} as a function of total exposure time under illumination with G = 2.0 × 10^{27} $cm^{-3}s^{-1}$ at 1.55 eV (800 nm): calculated curve and experimental points. For the values of parameters, see text. The saturated dangling bond density of 1 × 10^{19} cm^{-3} is shown in the figure (reproduced from Morigaki et al. [21]).

Stutzmann et al.[23] also made photoconductivity measurements under intense pulsed illumination, using a pulsed colliding pulse mode-locked (CPM) laser with a pulse width of 100 fs, a repetition frequency of 7 kHz, and a peak pulse power of 0.4 GW/ cm^2. Since they have not measured the relationship of σ_p^{-1} vs. N_s, we do not attempt to compare calculated results with experimental results. Here, we only point out that they observed the ESR spectrum of dangling bonds for this case at 300 K from which the dangling bond density was estimated to be 6 × 10^{17} cm^{-3} for average power density on the sample of 300 mW/ cm^2. They also measured the ESR spectra at 300 K under continuous (CW) illumination. We attempted to compare both spectra, as shown in Fig. 5, where the left peak and right peak of the ESR absorption derivative curve was normalized in Fig. 5(a) and (b), respectively. As seen from Fig. 5, the ESR line taken under intense pulsed illumination is more broadened than that taken under continuous illumination. Judging from the following deconvolution of the ESR line, this line broadening is related to the presence of hydrogen-related dangling bonds.

The ESR line observed under the intense pulsed illumination mentioned above is deconvoluted into two components a and b due to normal dangling bonds and hydrogen-related dangling bonds, respectively, as shown in Fig. 6(a). The obtained values of ESR parameters are given below: For normal dangling bonds (component a), the g-value, g, and the standard deviation of Gaussian spin-packet, σ, are g = 2.0053, σ = 6.2 G, respectively. The isotropic g-value is assumed for simplicity, because the anisotropic nature is weak. For hydrogen-related dangling bonds (component b), $g_{//}$ = 2.0066 and $g_{\perp}$= 2.0090, $A_{//}$ = 12 G and $A_{\perp}$= 3.2 G, $\sigma_{//}$ = 0.32 gauss and $\sigma_{\perp}$= 14.8 gauss, where $A_{//}$ and $A_{\perp}$ are the principal values of hyperfine interaction constants with hydrogen nucleus and $\sigma_{//}$ and $\sigma_{\perp}$ are the standard deviations of Gaussian spin-packet for two principal axes. The ratio of integrated intensity of component b to that of component a is 0.84. In order to examine their spin densities, we calculated r, q, s, w, r + q for the illumination condition for the observation of the ESR line, using the following values of parameters: G = 2.67 × 10^{30} $cm^{-3}s^{-1}$, r_0=1.0, q_0=0, B_0=1.78 × 10^4 s^{-1}, B_1= 2.67 × 10^5 s^{-1}, B_2=1 × 10^{-4} s^{-1}, B_3=0, B_4=1 × 10^{-2}

s^{-1}, $B_5 = 0$, $\beta = 3 \times 10^{-8}\,cm^3s^{-1}$ and $N_{d0} = 1 \times 10^{16}\,cm^{-3}$. For the values of parameters $C_d - C_5$, see Table 1. The result is shown in Fig. 7. For 2h of pulsed illumination under which the ESR line was observed, the exposure time is 5.04×10^{-6} s. For this time, we obtain r = 86.2, q = 46.6 and q/r = 0.54. The observed ratio of q to r is 0.84, as mentioned above. This is compared to the calculated value of 0.54, which is close to the observed value of 0.84. The observed dangling bond density of $6 \times 10^{17}\,cm^{-3}$ is about half of the calculated value of $1.3 \times 10^{18}\,cm^{-3}$ ($r + q = 1.3 \times 10^2$).

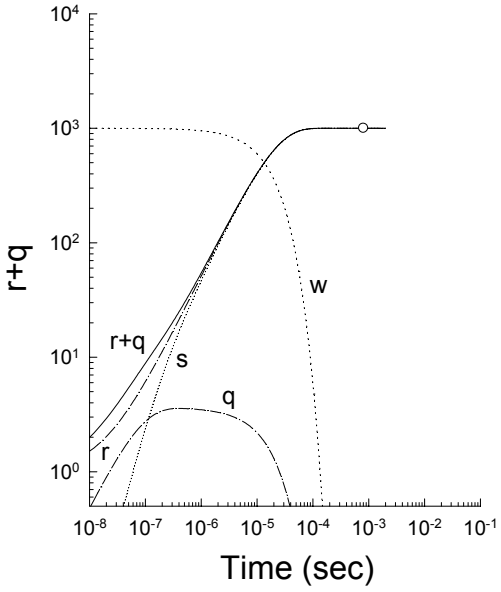

Fig. 9. Densities of total dangling bonds, r + q (solid line), normal dangling bonds, r (dotted line), hydrogen-related dangling bonds, q (solid line), metastable hydrogen atoms, s (dot-dashed line), and weak Si-Si bonds, w (solid line), relative to $N_{d0} = 1 \times 10^{16}$ cm^{-3} as a function of total exposure time under illumination with $G = 3.8 \times 10^{30}$ $cm^{-3}s^{-1}$ at 2.48 eV (500 nm): calculated curve and experimental points. For the values of parameters, see text. The saturated dangling bond density of 1×10^{19} cm^{-3} is shown in the figure (reproduced from Morigaki et al. [21]).

The ESR line observed after 4 h of continuous illumination by Stutzmann et al.[23] is fitted by a component due to normal dangling bonds, as shown in Fig. 6(b). The obtained values of ESR parameters are given below: $g_{//} = 2.0049$ and $g_{\perp} = 2.0062$, $\sigma_{//} = 3.8$ gauss and $\sigma_{\perp} = 7.9$ gauss. The result that only a component due to normal dangling bonds is observed in the ESR spectrum is consistent with our model [19].

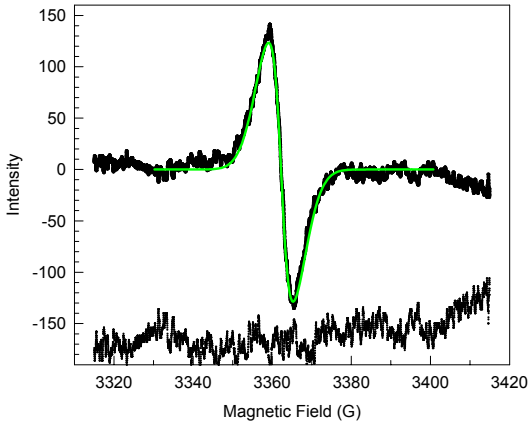

Fig. 10. Fitting of the observed ESR spectrum by a component due to normal dangling bonds in a light-soaked a-Si:H sample with 1 h of pulsed illumination at 1.55 eV (800 nm) shown in Fig. 8. The solid points and the solid curve are the observed ESR spectrum and the calculated ESR spectrum, respectively. The residual between the calculated ESR spectrum and the observed ESR spectrum is shown in the lower part of the figure with a scale twice extended compared to other curves.

The dangling bond density can be measured from ESR data. For intense pulsed illumination, ESR measurements have been performed for a-Si:H films prepared at 250 °C subject to intense pulsed illumination by a YAG optical parametric oscillator (OPO) laser system, in which pulse light was used with a width of 10 ns, a repetition frequency of 11 Hz and a power density of 100 mJ/cm^2 operating at either 2.48 eV (500 nm) or 1.55 eV (800 nm) [21]. The generation rate was $3.8 \times 10^{30}\,cm^{-3}s^{-1}$ and $1.4 \times 10^{30}\,cm^{-3}s^{-1}$ for illumination at 2.48 eV and $2.0 \times 10^{27}\,cm^{-3}s^{-1}$ for illumination at 1.55 eV. As examples of the kinetics of light-induced defect creation under intense pulsed illumination, we cite two figures from a previous paper [21], as shown in Fig. 8 for illumination at 1.55 eV(800 nm) and Fig. 9 for illumination at 2.48 eV (500 nm), i.e., r, q, s, w, and r + q vs. illumination time curves calculated using the values of parameters shown in Table 1. Experimental points are also shown in these figures. Illumination at 1.55 eV (800 nm) corresponds to a subbandgap excitation, i.e., in our model it is a direct excitation to create self-trapped holes in weak Si-Si bonds adjacent to Si-H bonds, because the level of self-trapped holes lies at 0.25 – 0.35 eV[25-27] above the mobility edge of valence band, depending on the hydrogen content of a-Si:H samples. Hence, the value of C_d for this

illumination is assumed to be larger than that of C_d for illumination corresponding to band to band excitation at 2.48 eV (500 nm).

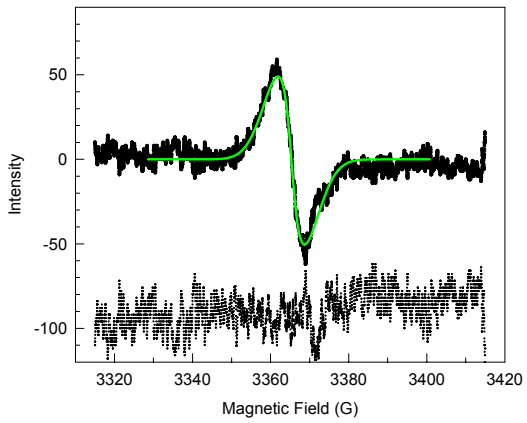

Fig. 11. Fitting of the observed ESR spectrum by a component due to normal dangling bonds in a light-soaked a-Si:H sample with 1 h of pulsed illumination at 2.48 eV (500 nm) shown in Fig. 9. The solid points and the solid curve are the observed ESR spectrum and the calculated ESR spectrum, respectively. The residual between the calculated ESR spectrum and the observed ESR spectrum is shown in the lower part of the figure with a scale twice extended compared to other curves. A signal seen in the residual part is due to the E' centre.

The ESR spectrum of an a-Si:H film subject to pulsed illumination at 1.55 eV (800 nm) for 1 h [21] is shown in Fig. 10. This spectrum is well fitted by a component with anisotropic g-values, $g_{//}$ = 2.0049 and $g_{\perp}$ = 2.0050, and anisotropic standard deviations of Gaussian spin-packet, $\sigma_{//}$ = 1.2 G and $\sigma_{\perp}$ = 4.8 G, as shown in Fig. 10. The second component due to hydrogen-related dangling bonds cannot be recognized. From Fig. 8, the ratio of the density of hydrogen-related dangling bonds to that of normal dangling bonds is estimated to be 0.31 for exposure time of 4×10^{-4} s (= illumination time of 1 h) (open circle in Fig. 8). However, as the peak intensity of the ESR absorption derivative depends on the line broadening, that of the ESR line due to hydrogen-related dangling bonds is small with 0.078 relative to that of the ESR line due to normal dangling bonds, taking into account that the line broadening of the former line is twice as large as that of the normal dangling bonds owing to the hyperfine interaction with hydrogen nucleus in the hydrogen-related dangling bonds [28]. Taking into account this small ratio, the peak intensity of the ESR line due to hydrogen-related dangling bonds may be within an experimental error. Hence, this is consistent with the observation mentioned above. The spin density after illumination mentioned above is 1×10^{18} cm^{-3} (the open circle in Fig. 8), being in a good agreement with the calculated spin density of 1.2×10^{18} cm^{-3} ($r + q = 1.2 \times 10^{2}$ in Fig. 8). For calculation, we assume that the spin density before illumination is 1×10^{16} cm^{-3}, because the ESR signal could not be observed before illumination owing to below the detection limit.

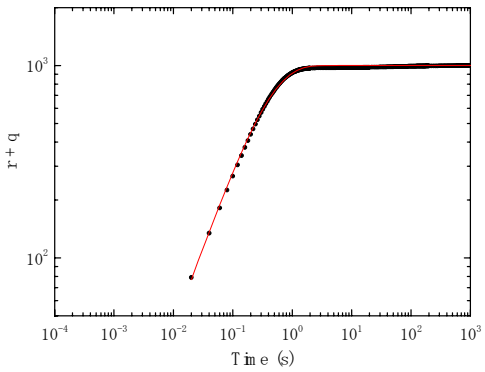

Fig. 12. Fitting of calculated curves of r + q vs. illumination time (solid lines) by a stretched exponential function given by eq. (31) (dotted line) for pulsed illumination at 1.55 eV (800 nm) shown in Fig. 8. See the text for detail.

The ESR spectrum of an a-Si:H film subject to pulsed illumination at 2.48 eV (500 nm) for 2 h [21] is shown in Fig. 11. This spectrum is well fitted by a component with anisotropic g-values, $g_{//}$ = 2.0050 and $g_{\perp}$ = 2.0051, and anisotropic standard deviations of Gaussian spin-packet, $\sigma_{//}$ = 1.2 G and $\sigma_{\perp}$ = 5.3 G, as shown in Fig. 11. The second component due to hydrogen-related dangling bonds cannot be recognized. From Fig. 9, the density of hydrogen-related dangling bonds is more than four orders of magnitude lower than that of normal dangling bonds for exposure time of 8×10^{-4} s (= illumination time of 2 h) (open circle in Fig. 9). Thus, the observation is consistent with the calculation. The observed dangling bond density is 1×10^{19} cm^{-3}, being in an exact agreement with the calculated one of 1×10^{19} cm^{-3}, as shown in Fig. 9.

4. Discussion

First, we discuss the saturation of light-induced dangling bond density at the long time limit of illumination time, as shown in Figs. 3(b), 8 and 9. This is correlated with a rapid decrease of weak bond density with increasing illumination time, i.e., the number of the potential sites for light-induced creation of dangling bonds is decreased, so that the light-induced dangling bond density reaches at a steady-state value. Thus, such

saturation behaviour is completely different from that for continuous illumination in which saturation occurs from balance between light-induced creation and annealing (termination by hydrogen) of dangling bonds[19]. Under weak illumination such as continuous illumination, the density of weak bonds does not change, keeping its density at an initial value, while under intense illumination such as pulsed illumination, the density of weak bonds changes with illumination time and quickly decreases at illumination time longer than 1 ms at $G = 5.7 \times 10^{27} cm^{-3}s^{-1}$, as shown in Fig. 3(b).

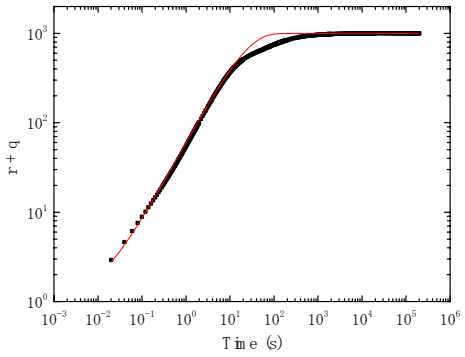

Fig. 13. Fitting of calculated curves of r + q vs. illumination time (solid lines) by a stretched exponential function given by eq. (31) (dotted line) for pulsed illumination at 2.48 eV (500 nm) shown in Fig. 9. See the text for detail.

The kinetics of light-induced defect creation is discussed in terms of a stretched exponential function as follows [29, 30]:

$$N_d(t) = N_{ss} - [N_{ss} - N_d(0)] \exp[-(t/\tau)^{\beta}], \quad (31)$$

where $N_d(t)$, N_{ss}, β and τ are the dangling bond density taken at a time t after illumination is switched on, the saturated dangling bond density (steady-state dangling bond density), a dispersive parameter and a characteristic time, respectively. The calculated curve of r + q vs. t can be fitted by a stretched exponential function, e.g., as shown in Fig.12 for illumination at 1.55 eV (800 nm) with $G = 2.0 \times 10^{25} cm^{-3}s^{-1}$ and Fig. 13 for illumination at 2.48 eV (500 nm) with $G = 3.8 \times 10^{24} cm^{-3}s^{-1}$ [21]. For the values of parameters used in the calculation, see Table 1. In Figs. 14 and 15 the obtained values of β and τ are plotted as a function of generation rate, G, respectively, where those of β and τ obtained for the case of continuous illumination are also shown. For the case of continuous illumination, two types of a-Si:H samples were used, which were prepared at 250 °C by plasma-enhanced chemical vapour deposition (PECVD) using a gas mixture of SiH_4 and H_2 in Ecole Polytechnique [29] and Yamaguchi University [30]. In these figures are shown calculated results of β and τ for continuous illumination, using the following values of parameters: $C_d = 2 \times 10^{-15} cm^3\ s^{-1}$, $C_1 = 4 \times 10^{-31} cm^6\ s^{-1}$, $C_2 = 1.28 \times 10^{-21} cm^3\ s^{-1}$, $C_3 = 0$, $C_4 = 0$, $C_5 = 0$, and $N_{d0} = 1 \times 10^{16}\ cm^{-3}$. From Fig. 14 it is found that the values of β for intense pulsed illumination are apart from the tendency of β for weak continuous illumination This indicates that the kinetics of light-induced defect creation is different between weak and intense illumination. On the other hand, the values of τ decrease with increasing G, as seen from Fig.15. The same tendency of τ with G is seen for weak and intense illumination. Under intense illumination, a number of dangling bonds and metastable hydrogen atoms are created, so that mutual distance between a dangling bond and a metastable hydrogen atom becomes short and their lifetime distribution becomes narrow around the average lifetime. This suggests that β becomes large being close to 1. This is consistent with the observation, as shown in Fig. 14. The result that τ becomes short under intense illumination, as shown in Fig. 15, is quite reasonable from the above viewpoint.

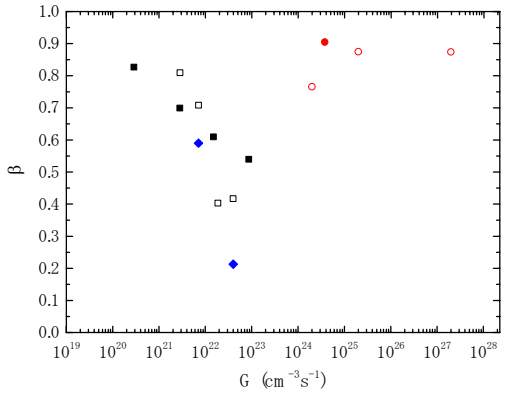

Fig. 14. β vs. G. Open circles: Calculated results for pulsed illumination at 1.55 eV (800 nm), closed circle: Calculated results for pulsed illumination at 2.48 eV (500 nm) [21]. For the values of parameters used for the calculations, see the text. Open squares: Experimental results for samples prepared in Ecole Polytechnique for continuous illumination (cited from Morigaki et al.[29]), closed diamonds: Experimental results for samples prepared in Yamaguchi university for continuous illumination(cited from Morigaki et al.[30]). Closed squares: Calculated results (cited from Morigaki et al.[30]) which are obtained, using the following values of parameters: $C_d = 2 \times 10^{-15} cm^3\ s^{-1}$, $C_1 = 4 \times 10^{-31} cm^6\ s^{-1}$, $C_2 = 1.28 \times 10^{-21} cm^3\ s^{-1}$, $C_3 = 0$, $C_4 = 0$, $C_5 = 0$, and $N_{d0} = 1 \times 10^{16}\ cm^{-3}$. See the text for detail.

Second, we discuss related defects, i.e., self-trapped holes and hydrogen-related dangling bonds in a-Si:H. The self-trapping of holes in weak Si-Si bonds adjacent to Si-H bonds plays an important role in the light-induced

creation of dangling bonds. The existence of such weak Si-Si bonds was first suggested on the basis of the following speculations [8]: The bond strength of the Si-H bond is stronger than that of the normal Si-Si bond and the electronegativity of hydrogen is larger than that of silicon. As a consequence, the bonding orbital electrons of the central Si atom will be more localized towards the stronger bond, i.e., the Si-H bond, than towards other bonds. This suggestion has been confirmed by an abinitio molecular dynamics computer simulation by Yonezawa et al. [31].

The self-trapping of holes in such specific weak Si-Si bonds has also been confirmed by optically detected electron-nuclear double resonance (ODENDOR) measurements [32-35], i.e., the ENDOR signal due to hydrogen nucleus has been observed at 7 K in high-quality a-Si:H films.

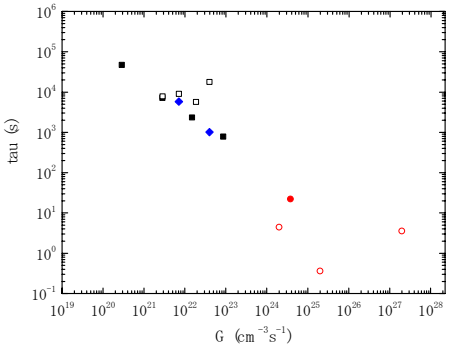

Fig. 15. τ vs. G. The symbols used in the figure are the same as those in Fig. 14. The results for continuous illumination are cited from Morigaki et al.[29, 30]. Calculated results are obtained, using the same values of parameters as those in Fig. 14. See the text for detail.

Other evidence for self-trapping of holes in such specific weak Si-Si bonds at low temperatures has been presented in a previous paper [35]. Here, we show very recent experimental results of modulated infrared (IR) absorption measurements, i.e., IR absorption measurements under optical excitation, in which self-trapping of holes in such specific weak Si-Si bonds is suggested. The observation that the IR absorption intensity due to the stretching mode of the Si-H bond vibration at 2000 cm^{-1} is decreased by optical excitation is accounted for in terms of the dipole moment for the vibration mode [36], i.e., in our model holes are self-trapped in the specific weak Si-Si bond adjacent to the Si-H bonds and then the dipole moment for the vibration mode becomes small. Very recently, Oheda [37] made detailed measurements of modulated IR absorption measurements as functions of density of HSi-Si$_3$ unit and steady-state photoluminescence (PL) intensity in a-Si:H and related alloys at 11 K. He observed that the decrease of the IR absorption intensity at 2000 cm^{-1} under optical excitation is correlated with the density of HSi-Si$_3$ unit and PL intensity associated with triplet excitons (1 ms lifetime component) and distant electron-hole pair recombination (10 μs lifetime component), particularly the PL state associated with the 1 ms lifetime component exhibits a much stronger self-trapping nature than the PL state associated with the 10 μs lifetime component at low temperatures. This result is reasonable, because the PL state of the 1 ms lifetime component is a triplet self-trapped exciton [38], while the PL state of the 10 μs lifetime component is a distant electron-hole pair, in which the hole is self-trapped, but the electron is a tail electron more extended than the self-trapped hole. This observation indicates that self-trapping of holes is correlated with the Si-H bond. Hence, this is consistent with our model that a hole is self-trapped in a weak Si-Si bond adjacent to a Si-H bond.

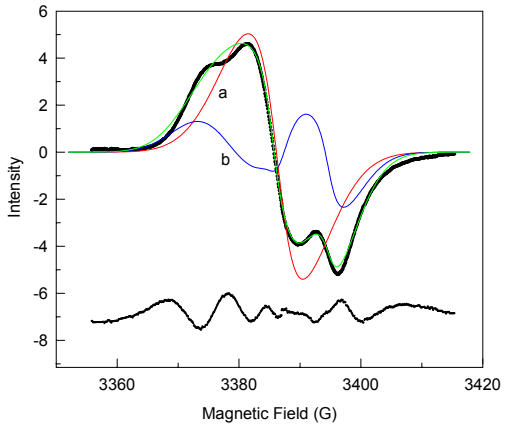

Fig. 16. Deconvolution of the ESR spectrum observed by Astakhov et al.[42] into two components due to dangling bonds a and hydrogen-related dangling bonds b in an electron-irradiated a-Si:H sample (cited from Astakhov et al. [42]). The solid points and the solid curve are the observed ESR spectrum and a superposition of dashed curves a and b, respectively. The residual between the calculated ESR spectrum and the observed ESR spectrum is shown in the lower part of the figure with a scale twice extended compared to other curves.

The presence of hydrogen-related dangling bonds is a consequence of our model for light-induced defect creation in a-Si:H. For high-quality a-Si:H films, the density of light-induced hydrogen-related dangling bonds is lower than that of normal dangling bonds, particularly the peak intensity of their ESR absorption derivatives is about four times smaller than their density relative to normal dangling bonds owing to their line broadening, as

mentioned before. For low-quality a-Si:H films, we have obtained evidence for the presence of hydrogen-related dangling bonds from the deconvolution of the ESR line [28, 39] and the ENDOR measurement [40, 41]. Very recently, hyperfine structure due to hydrogen nucleus has been observed in the dangling bond ESR spectrum for electron-irradiated a-Si:H films [42]. We attempted to deconvolute the ESR spectrum observed by Astakhov et al.[42] into two components due to normal dangling bonds and hydrogen-related dangling bonds, as shown in Fig. 16. From the deconvolution, the values of ESR parameters were determined as follows: For normal dangling bonds, $g_{//} = 2.0043$, and $g_{\perp} = 2.0048$, $\sigma_{//} = 1.8$ gauss and $\sigma_{\perp} = 6.9$ gauss and for hydrogen-related dangling bonds, $g_{//} = 2.0021$, and $g_{\perp} = 2.0055$, $A_{//} = 8.9$ G, and $A_{\perp} = 16.9$ G, $\sigma_{//} = 1.0$ gauss and $\sigma_{\perp} = 5.3$ gauss, where $A_{//}$ and $A_{\perp}$ are the principal values of hyperfine interaction constants. From our calculation [28] of the relationship of $A_{//}$ and $A_{\perp}$ vs. the distance between the dangling bond site and hydrogen, R, R is derived with the above values of $A_{//}$ and $A_{\perp}$ to be 2.2 Å. This is compared with R = 2.1 – 2.2 Å for low-quality a-Si:H films[28, 39] and R = 2.7 Å for hydrogen-complex in H-implanted crystalline silicon [43] (Fig. 17). The observation of hyperfine structure by Astakhov et al.[42] may provide evidence for the existence of the hydrogen-related dangling bond in electron-irradiated a-Si:H. The issue of hydrogen-related dangling bonds has also been discussed in a previous paper [44].

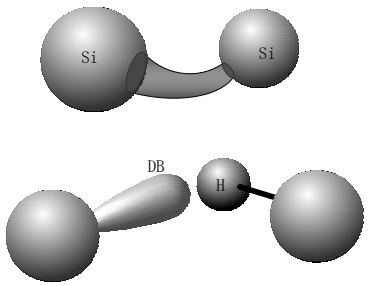

Fig. 17. Atomic configuration of the vacancy-hydrogen complex in crystalline Si proposed by Nielsen et al. [43].

Third, we consider the recent important observation of hydrogen-pairs in nuclear magnetic resonance (NMR) measurements at 7-10 K in light-soaked a-Si:H samples [45, 46]. This has a significant importance for elucidating the mechanism of light-induced defect creation in a-Si:H. Thus, this is a key factor to examine whether the model proposed until now successfully operates or not to account for the light-induced defect creation. In our model, the concentration of hydrogen-pairs created by illumination has been calculated on the basis of Eqs. (6) – (8) and the result is in a good agreement with the experimental result [47]. However, it has been pointed out in our model that the C_4 term in Eqs. (1) – (3) (the A_4 term in Eqs. (6) – (8)) is required not to be zero, i.e., $C_4 \neq 0$, for the light-induced creation of hydrogen-pairs. This means that the concentration of light-induced dangling bonds does not saturate with increasing illumination time or does not easily saturate by normal illumination condition under continuous illumination. The concentration of light-induced hydrogen-pairs has not been measured as a function of illumination time and the illumination-time dependence of light-induced dangling bonds has also not been reported for the samples used in the observation of light-induced hydrogen-pairs by NMR. Further investigations for these issues as well as for other a-Si:H samples, e.g., exhibiting the saturation of light-induced dangling bond density, are required. Further, the interaction between dangling bonds as paramagnetic species and hydrogen-pairs is required from the measurement of spin-lattice relaxation times of light-induced hydrogen-pairs [45]. In our model, a dangling bond may be located from hydrogen-pairs with a distance of ~13 Å under illumination [19]. Thus, this dangling bond acts as a rapid relaxation centre for hydrogen-pairs [47].

Finally, we comment about the so-called microscopic constraints which should be required by any model for light-induced defect creation in a-Si:H, e.g.,Branz [15] mentioned that the ESR data would exclude the entire class of models involving local motion of hydrogen as a step in the creation of dangling bonds, where the ESR data [48, 49] mean from the ESR hyperfine studies that no hyperfine structure is found in the ESR spectra and also from pulsed ESR that dangling bonds are not normally found within about 4 Å from hydrogen atoms. It has already been pointed out that this is incorrect (see appendix of ref.[19]). As mentioned above, the density of hydrogen-related dangling bonds is much lower than that of normal dangling bonds for high-quality a-Si:H films, so that the ESR signal of hydrogen-related dangling bonds has not been observed owing to the limited detection sensitivity.

5. Conclusions

The experimental results taken from the literatures on the kinetics of light-induced defect creation under intense pulsed illumination in a-Si:H are reviewed and discussed in terms of our model, taking into account the bimolecular recombination of carriers for G more than 1×10^{27} $cm^{-3}s^{-1}$. The calculated result based on this model is compared with the experimental result of Tzanetakis et al. [22]. For Stutzmann et al' experiment[23] at $G = 5 \times 10^{24}$ $cm^{-3}s^{-1}$, the monomolecular recombination case was experimentally confirmed from comparison between photoconductivity and ESR (spin density), so that the

calculated result based on the monomolecular recombination is compared with photoconductivity vs. illumination time. In these comparisons, the experimental results are consistent with the calculated results. ESR spectra observed by Stutzmann et al. [23] and by Morigaki et al. [21] are deconvoluted into two components due to normal dangling bonds and hydrogen-related dangling bonds. The results of the ratio of integrated intensities of two components are compared with the calculated result obtained from the calculated curve of r and q vs. illumination time. The calculated results are consistent with the observations. The relationship of β and τ vs. G for intense illumination can be understood in terms of our model. A difference in the density of weak Si-Si bonds between weak and intense illumination is that it does not change with illumination time for the former, while it changes with illumination time and quickly decreases with illumination time above a certain illumination time for the latter. Related defects, i.e., hydrogen-related dangling bonds, self-trapped holes and hydrogen pairs, are discussed. Some evidence for the existence of hydrogen-related dangling bonds and self-trapped holes is presented, being also consistent with our model for light-induced defect creation in a-Si:H.

References

[1] D. L. Staebler, C. R. Wronski, Appl. Phys. Lett. **31**, 292 (1977).
[2] K. Shimakawa, A. Kolobov, S. R. Elliott, Adv. Phys. **44**, 475 (1995).
[3] H. Fritzsche, Mat. Res. Soc. Symp. Proc. **467**, 19 (1997).
[4] M. Stutzmann, Mat. Res. Soc. Symp. Proc. **467**, 37 (1997).
[5] K. Morigaki, Physics of Amorphous Semiconductors, World Scientific, Singapore and Imperial College Press, London (1999).
[6] J. Singh, K. Shimakawa, Advances in Amorphous Semiconductors, Taylor & Francis, London (2003).
[7] T. Shimizu, Jpn. J. Appl. Phys. **43**, 3257 (2004).
[8] I. Hirabayashi, K. Morigaki, S. Nitta, Jpn. J. Appl. Phys. **19,** L357 (1980).
[9] H. Dersch, J. Stuke, J. Beichler, Appl. Phys. Lett. **38,** 456 (1981).
[10] M. Stutzmann, W. B. Jackson, C. C. Tsai, Phys. Rev. **B32** (1985) 23.
[11] K. Morigaki, Jpn. J. Appl. Phys. **27,** 163 (1988).
[12] K. Morigaki, J. Non-Cryst. Solids **141,** 166 (1992).
[13] C. Godet, P. Roca i Cabarrocas, J. Appl. Phys. **80**, 97 (1996).
[14] C. Godet, J. Non-Cryst. Solids **227-230**, 272 (1998).
[15] H. M. Branz, Phys. Rev. B59, 5498 (1999).
[16] N. Kopidakis, E. A. Schiff, J. Non-Cryst. Solids **266-269**,415 (2000).
[17] C. Longeaud, D. Roy, O. Saadane, Phys. Rev. B**65**, 085206 (2002).
[18] H. M. Branz, Solar Energy Mat. **78**, 425 (2003).
[19] K. Morigaki, H. Hikita, Phys. Rev. B **76**, 085201 (2007).
[20] K. Morigaki, H. Hikita, J. Non-Cryst. Solids **299-302**,455 (2002).
[21] K. Morigaki, H. Hikita, H. Takemura, T. Yoshimura, C. Ogihara, Philos. Mag. Lett. **83**, 341 (2003).
[22] P. Tzanetakis, N. Kopidakis, H. Fritzsche, J. Non-Cryst. Solids **198-200**, 276 (1996).
[23] M. Stutzmann, M. C. Rossi, M. S. Brandt, Phys. Rev. **B50**, 11592 (1994).
[24] P. Stradins, M. Kondo, A. Matsuda, J. Non-Cryst. Solids **266-269,** 405 (2000).
[25] I. Hirabayashi, K. Morigaki, J. Non-Cryst. Solids **59 & 60**, 433 (1983).
[26] K. Morigaki, H. Takenaka, I. Hirabayashi, M. Yoshida, Tetrahedrally-Bonded Amorphous Semiconductor*s*, edited by D. Adler and H. Fritzsche, Plenum Pub. Corp., New York (1985) p.221.
[27] M. Yamaguchi, K. Morigaki, J. Non-Cryst. Solids **137&138**, 57 (1991).
[28] H. Hikita, K. Takeda, Y. Kimura, H. Yokomichi, K. Morigaki, J. Phys. Soc. Japan **66**, 1730 (1997).
[29] K. Morigaki, K. Takeda, H. Hikita, P. Roca i Cabarrocas, Solid State Commun. **142**, 232 (2007).
[30] K. Morigaki, K. Takeda, H. Hikita, C. Ogihara, P. Roca i Cabarrocas, J. Non-Cryst. Solids **354**, 2131 (2008).
[31] F. Yonezawa, S. Sakamoto, M. Hori, J. Non-Cryst. Solids **137&138**, 135 (1991).
[32] M. Kondo, K. Morigaki, J. Non-Cryst. Solids **114**, 408 (1989).
[33] M. Kondo, K. Morigaki, in Proc. Int. Conf. Physics of Semiconductors, edited by E. M. Anastassakis and J. D. Joannopoulos ,World Scientific, Singapore (1990) p. 2083.
[34] M. Kondo, K. Morigaki, J. Non-Cryst. Solids **137-138**, 247 (1991).
[35] K. Morigaki, H. Hikita, M. Kondo, J. Non-Cryst. Solids **190**, 38 (1995).
[36] Z. Vardeny, M. Olszatier, J. Non-Cryst. Solids **97&98**, 109 (1987).
[37] H. Oheda, J. Appl. Phys. **101**, 0537111 (2007).
[38] M. Yoshida, K. Morigaki, J. Phys. Soc. Japan **58**, 3371 (1989).
[39] K. Morigaki, H. Hikita, M. Yamaguchi, Y. Fujita, J. Non-Cryst. Solids **227-230**, 338 (1998).
[40] H. Yokomichi, K. Morigaki, Solid State Commun. **63**, 629 (1987).
[41] H. Yokomichi, K. Morigaki, Phil. Mag. Lett. **73**, 283 (1996).
[42] O. Astakhov, R. Carius, A.Lambertz, Yu. Petrusenko, V. Borysenko, D. Barankov, F. Finger, J. Non-Cryst. Solids **354**, 2329 (2008).
[43] B. Bech Nielsen, P. Johannesen, P. Stallinga, K. Bonde Nielsen, Phys. Rev. Lett. **79**,1507 (1997).
[44] K. Morigaki, Proc. Third Int. Conf. Optical, Optoelectronic and Photonic Materials and Applications, Edmonton, Canada (2008). Phys.

Stat. Solidi C, in press.
[45] T. Su, P. C. Taylor, G. Ganguly, D. E. Carlson, Phys. Rev. Lett. **89**, 015502 (2002).
[46] T. Su, P. C. Taylor, G. Ganguly, D. E. Carlson, J. Non-Cryst. Solids **338**-**340**, **3**57 (2004).
[47] K. Morigaki, H. Hikita, Solid State Commun. **136**, 616 (2005).
[48] J. Isoya, S. Yamasaki, H. Okushi, A. Matsuda, K. Tanaka, Phys. Rev. B47, 7013 (1993).
[49] S. Yamasaki, J. Isoya, J. Non-Cryst. Solids **164-166**, 169 (1993).

*Corresponding author: k.morigaki@yacht.ocn.ne.jp